JOURNAL OF GEOPHYSICAL RESEARCH, VOL. 112, A06206, doi:10.1029/2006JA012061, 2007

Chorus source properties that produce time shifts and frequency range differences observed on different Cluster spacecraft

J. Chum,[1] O. Santolík,[2,3] A. W. Breneman,[2] C. A. Kletzing,[2] D. A. Gurnett,[2] and J. S. Pickett[2]

Received 8 September 2006; revised 20 March 2007; accepted 27 March 2007; published 2 June 2007.

[1] We present an explanation of frequency range differences and time shifts between corresponding chorus elements of whistler mode chorus which have been recently observed on multiple Cluster spacecraft. We show that a nonmoving or quasi-static source that emits waves in a relatively narrow interval of wave normal angles and that varies both the wave normal angle and frequency during the generation of a single chorus element can reproduce these observations. To validate this model, we perform a ray tracing analysis from a source located close to the geomagnetic equator to simulate the dispersion properties and relative timing of the chorus elements observed at different spacecraft. We demonstrate that the ray tracing simulation leads to patterns which are very similar to those observed.

Citation: Chum, J., O. Santolík, A.W. Breneman, C. A. Kletzing, D. A. Gurnett, and J. S. Pickett (2007), Chorus source properties that produce time shifts and frequency range differences observed on different Cluster spacecraft, *J. Geophys. Res.*, *112*, A06206, doi:10.1029/2006JA012061.

1. Introduction

[2] Chorus counts among the most intense natural electromagnetic emissions generated in the whistler mode in the inner magnetosphere outside the plasmapause. It consists of narrowband tones tones usually rising (sometimes falling) in frequency on the timescale of several tenths of a second. Near the magnetic equator, chorus usually occurs in two distinct frequency bands separated by a narrow gap near one half of equatorial electron cyclotron frequency $\omega_{ce,eq}$ [*Tsurutani and Smith*, 1974], the upper band with $\omega/\omega_{ce,eq} \sim 0.5-0.75$ and the lower band in the frequency range $\omega/\omega_{ce,eq} \sim 0.2-0.45$, where ω is the wave angular frequency. *Tsurutani and Smith* [1974] and *Anderson and Maeda* [1977] found that the onset of the emissions coincided with the injection of substorm electrons with energies from units to tens of keV that interact with whistler mode waves through the cyclotron resonance [*Andronov and Trakhtengerts*, 1964; *Kennel and Petschek*, 1966].

[3] Recent Poynting flux measurement on Polar [*LeDocq et al.*, 1998] and the Cluster satellite [*Parrot et al.*, 2003a, 2003b; *Santolík et al.*, 2004b, 2005] have confirmed the previous suggestion by *Helliwell* [1967, 1969] that the chorus source is located close to the magnetic equatorial plane, the dimension along magnetic field line being up to several thousands of kilometers, thus expanding up to 3 degrees from the magnetic equator. The cross-correlation of spectrograms recorded on different Cluster satellites in the source region during a geomagnetic storm has shown that the transverse dimension (with respect to magnetic field) of the sources is about 100 km in the case of lower-band chorus [*Santolík and Gurnett*, 2003; *Santolík et al.*, 2004a].

[4] The detailed understanding of the chorus generation mechanism is still a subject of intense research. Several authors have attempted to explain the main properties of chorus emission, such as the recurrence rate and the slope of chorus elements. *Trakhtengerts* [1995, 1999] introduced the theory of a backward wave oscillator in the ELF/VLF frequency band. According to this theory, a step-like electron distribution function, which is formed as a result of the development of a cyclotron instability, leads to wave generation in the form of discrete elements with rising frequency. *Nunn et al.* [1997] considered a strong nonlinear phase trapping of cyclotron resonant electrons as the underlying mechanism behind the structure of VLF chorus. *Omura and Summers* [2006] showed that bunching of electrons in the phase of their cyclotron motion causes chorus generation. They pointed out that the change of wave frequency is related to the inhomogeneity of the geomagnetic field in the equatorial region. They also discussed the acceleration of trapped electrons.

[5] Originally, the properties of chorus waves have been studied under the assumption of ducted propagation of the emission from the source. However, the observed evolution of the wave normal angle as a function of latitude [*Santolík et al.*, 2003] and the first identification of magnetospherically reflected (MR) chorus described by *Parrot et al.*

[1]Institute of Atmospheric Physics, Academy of Sciences of the Czech Republic, Prague, Czech Republic.
[2]Department of Physics and Astronomy, University of Iowa, Iowa City, Iowa, USA.
[3]Permanently at Faculty of Mathematics and Physics, Charles University, Prague and IAP/ASCR, Prague, Czech Republic.

0148-0227/07/2006JA012061$09.00

[2003a, 2004] show that in many cases, no ducts exist, and that, at least outside of the source region, chorus can propagate obliquely with respect to magnetic field lines. *Horne and Thorne* [2003] studied the resonant interactions of the relativistic electrons with obliquely propagating whistler mode chorus at higher geomagnetic latitudes. They showed that these interactions can lead both to electron acceleration and precipitation.

[6] Multipoint observation performed by the Cluster satellites have revealed a new and interesting feature of chorus emission: a single chorus element (or group of elements) can have shifts in time and different upper and lower frequency limits observed on each of the Cluster spacecraft. This phenomenon was first pointed out by *Gurnett et al.* [2001]. *Inan et al.* [2004] have put forward a model in which waves generated from a rapidly moving point-like source emitting in a large span of wave normal angles up to the resonance cone experience a considerable Doppler shift. This could cause the observed frequency difference between individual discrete elements observed on different Cluster spacecraft. The speeds at which the sources must move along the field lines are, according to this theory, comparable to the parallel velocity of gyroresonant electrons or the wave group velocity, i.e., of the order of one tenth of the speed of light.

[7] In the companion paper [*Breneman et al.*, 2007] we have shown that some of the observed time and frequency shifts can alternatively result from a stationary source combined with limited accessibility of the spacecraft positions for whistler mode waves emitted from a source region located close to the equatorial plane. In that paper we have demonstrated that the position of this source region can be found using a reverse ray-tracing technique started from the observation points. We have further shown that large time shifts ($\approx$0.2 s) between the corresponding elements observed on different spacecraft cannot be explained by a stationary source radiating at the same time at different wave normal angles.

[8] A possible explanation of these large time shifts is proposed in the present paper. The explanation is demonstrated on an example of falling elements. It is based on the idea that a source radiates in a relatively narrow interval of wave normal angles, and that both the wave normal angle and frequency change with time during the generation of a single element.

[9] We also present a simulation of rising tones. A small time shift of several tens of ms is observed between corresponding elements on different spacecraft in this case. Our simulation, based on the forward ray-tracing, confirms the results [*Breneman et al.*, 2007] that a frequency shift can arise from the fact that waves of different frequencies that originally formed a single element in the source propagate to different spacecraft positions.

[10] Our model does not use the assumption of rapidly moving sources as does the model of *Inan et al.* [2004]. However, with the available data we are unable to decide which solution is more appropriate, or even whether any of them is realistic. The purpose of the present paper is to propose an alternative explanation for the time and frequency shifts between corresponding chorus elements observed at different points in space, but we cannot state that our model is unique nor that we consider our model better than the earlier model of *Inan et al.* [2004].

[11] Section 2 shows the observations, section 3 describes our hypothesis on properties of the chorus sources, section 4 shows examples of simulation results with implications for resonating electrons, section 5 discusses these results, and section 6 presents brief conclusions.

2. Observations

[12] Figure 1 presents an example of a simultaneous observation at two different Cluster spacecraft of the same chorus elements shifted in time and with different upper and lower frequency limits. These time-frequency spectrograms of one component of the electric field were recorded by Cluster 1 and 2 on 27 November 2000 by the Wideband Data (WBD) receiver (for details of operation, see *Gurnett et al.* [1997]). This event has been discussed previously by *Gurnett et al.* [2001] and *Inan et al.* [2004]. Onboard measurements of the electron cyclotron frequency by the FGM instrument [*Balogh et al.*, 2001] give $\omega_{ce}/2\pi \sim$12.6 kHz. We observe chorus emissions in the frequency range from $\approx$6.5 kHz to $\approx$9.3 kHz, so their normalized frequencies cover an interval $0.516 \leq \omega/\omega_{ce} \leq 0.738$ which corresponds to the upper-band chorus. The plasma density of $\sim$22 particles/cm^3 estimated from measurements of the WHISPER instrument [*Décréau et al.*, 2001] gives a plasma frequency $\omega_p/2\pi \sim$42 kHz. At the time of the observation, the geomagnetic coordinates of the spacecraft were as follows: SC1 was located at L = 3.845, MLAT = $-0.808°$, MLT = 6.693 hours, and SC2 was at L = 3.856, MLAT = $-3.3512°$, MLT = 6.682 hours. The positions of the spacecraft in the meridian plane are marked in Figures 2 and 4 and were located very close to the magnetic equator.

[13] The time interval in which we found several of these one-to-one correspondences of chorus elements lasted from $\sim$1312:45 to $\sim$1314:00. Outside of this time interval, we observed a similar difference in the frequency range of emissions recorded by these two spacecraft, but there was no clear correspondence of individual chorus elements observed on different spacecraft. The elements again show a clear one-to-one correspondence around 1331:50, when the spacecraft were much further from the equator.

[14] Note that it is sometimes difficult to distinguish whether we observe a single chorus element or two or more elements that occur almost at the same frequency and time. For example, relatively sharp falling elements are often observed together with rather fuzzy rising elements in Figure 1. In the case of fuzzy rising elements, the elements are usually observed at about the same time on both spacecraft at a given fixed frequency.

[15] In the case of falling elements, at a given fixed frequency, the corresponding element is observed about $\sim$250 ms sooner on Cluster 2 than on Cluster 1 despite the fact that Cluster 1 is closer to the geomagnetic equator than Cluster 2. This is a very surprising fact, seemingly inconsistent with the assumption that the source region is located close to the geomagnetic equator. Moreover, the corresponding time shift is relatively high, much larger than the parallel separation distance of the two spacecraft divided by the estimated group velocity of parallel propagation of the whistler mode waves. Thus the time shift cannot be

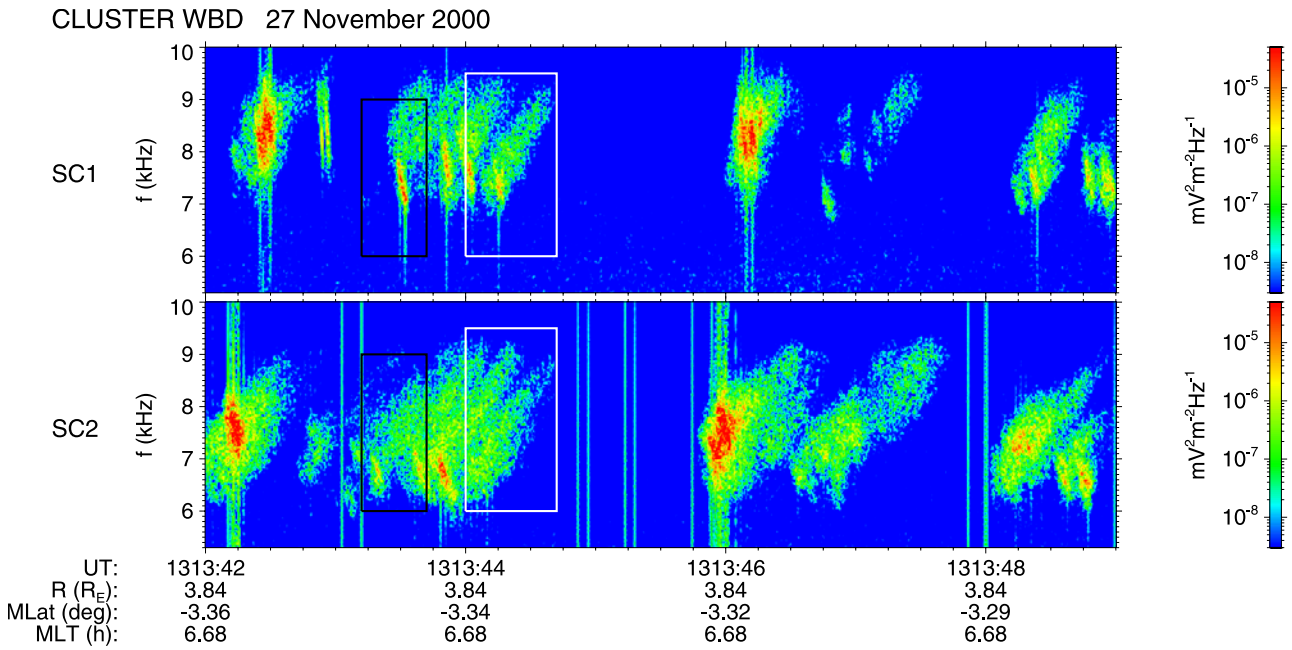

Figure 1. Frequency-time spectrograms obtained by the WBD instruments on board Cluster 1 (SC1) and Cluster 2 (SC2) on 27 November 2000 from 1313:42 to 1313:49 UT. On the bottom, coordinates (R-radial distance, MLat-magnetic dipole latitude, MLT-magetic local time) are given for Cluster 2. Groups of falling elements and rising chorus elements are observed. There is a clear one-to-one correspondence between the chorus elements observed on both satellites, but the frequency range on Cluster 1 is higher. Two frequency-time subintervals, shown by black and white rectangles, respectively, are used for further analysis.

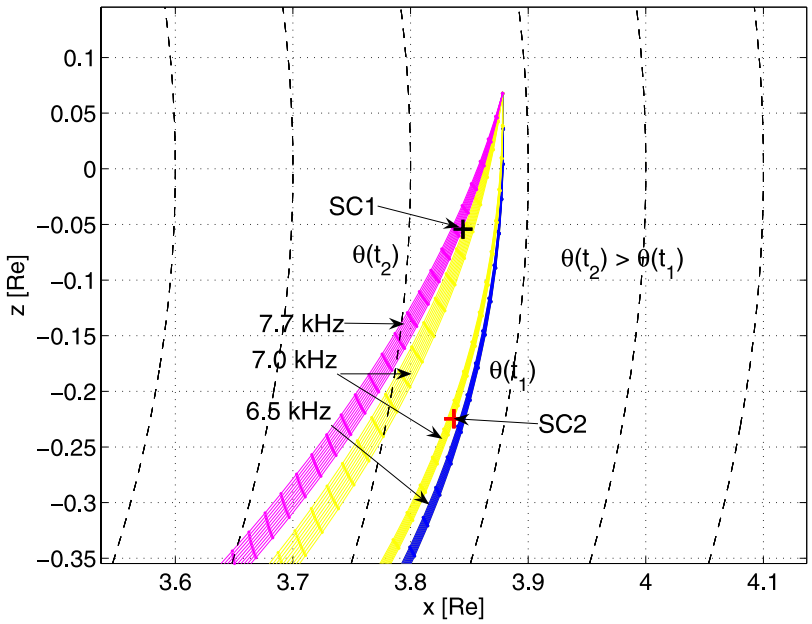

Figure 2. A schematic view in meridian $Z_{SM} - X_{SM}$ plane of the chorus source used in the simulation for falling elements. Figure displays the ray trajectories (solid lines) for different frequencies (distinguished by colors) at different times t1 and t2, separated by 250 ms, as observed on Cluster 1 (SC1) and Cluster 2 (SC2). The dashed lines represent dipole magnetic field lines. A narrow interval of emission angles θ (with a width of $\approx 3^\circ$) is used, centered at an angle which increases with time from 0.25 θ_R at time t1 to 0.65 θ_R at time t2 (θ_R is the resonance angle, see the text). As the emission angle increases in time, Cluster 2 observes the falling element sooner than Cluster 1 which is closer to the geomagnetic equatorial plane where $Z_{SM} = 0$.

explained solely by equatorward propagation from a more distant source below the equator. This time shift of the observations provides a key property for testing the model presented here.

3. Hypothesis on Properties of Chorus Source

[16] First, we clarify how we quantify the time shift between the corresponding chorus elements recorded on different spacecraft. We define the time shift as the time difference between the maxima of the wave intensity at a given fixed frequency for a chorus element observed on two spacecraft. This is a different approach from that which has been used by *Inan et al.* [2004], who calculate the time delay from the Doppler-shifted frequencies. This leads to slightly different values of the time shift for the same case. The reason for the difference is that for the hypothesis discussed in the present paper, we do not consider the Doppler shift to be responsible for the observed frequency range differences. Instead, we assume that each chorus element is generated over a broad frequency range and only a subinterval of the original frequency range reaches a given spacecraft due propagation effects. Because the two spacecraft have different positions, they will observe different frequency subintervals because not all rays can reach both spacecraft. This will cause a chorus element as seen on one spacecraft to appear to be frequency shifted relative to the same element on another spacecraft.

[17] Second, we assume that particles interacting with chorus waves in their source region roughly satisfy the first-order cyclotron resonance condition,

$$\omega - k_{\|} \cdot v_{\|} = \omega_{ce}/\gamma \ , \tag{1}$$

where ω is the wave angular frequency, $k_{\|}$ is the parallel component of wave vector $\mathbf{k}$ ($k_{\|} = k\cos\theta$, θ is angle between the wave vector and the ambient magnetic field), $v_{\|}$ is parallel component of velocity v of resonant particles ($v_{\|} = v\cos\alpha$, α is a pitch angle), $\omega_{ce} = eB_0/m$ is the nonrelativistic electron cyclotron frequency and γ is the Lorentz factor $\gamma = c/\sqrt{c^2 - v^2}$. The resonance condition (1) defines the parallel component $k_{\|}$ of the wave vector for given ω, v, and α.

[18] In addition, $k_{\|}$ must satisfy the wave dispersion relation. Under the cold plasma approximation [see, e.g., *Gurnett and Bhatacharjee*, 2005], $k_{\|}$ depends on the cyclotron frequency ω_{ce} (related to the ambient magnetic field), plasma frequency ω_p (related to the plasma density), angular wave frequency ω, and on the wave normal angle θ. For whistler mode waves in our range of frequencies, this approximation of the dispersion relation reads

$$\omega_p^2\omega + (\omega - \omega_{ce}\cos\theta)\left(\frac{c^2k_{\|}^2}{\cos^2\theta} - \omega^2\right) = 0, \tag{2}$$

where c is the speed of light.

[19] For the case of chorus, we have to consider that the wave changes its frequency during the generation process of a single element. The frequency drift can be a consequence of changes in velocity v and pitch angle α of the unstable particle population. These variations can also be accompanied by changes of the wave normal angle of the generated waves to keep the particles in resonance with a wave of changing frequency.

[20] Let us assume that, at a given time, the waves are generated in a narrow interval of wave normal angles θ and in a narrow interval of frequencies and that both wave normal angles and frequencies increase with time during the generation of a single chorus element in agreement with equations (1)–(2). Since waves with different initial angles propagate along different trajectories, the source can illuminate different satellites at different times. The rate of change of the characteristic angle θ is then responsible for the time shifts. The slower the θ variation, the larger the time shifts are. The widths of the intervals of wave normal angles and frequencies then determine the widths (thicknesses) of the observed chorus elements in the time-frequency plane.

4. Simulation Results

[21] To verify that the above proposed model explains the observations we will calculate the times of arrival for waves at different frequencies which would be observed by spacecraft at different given positions. For simplicity, we will assume a point source from which we will launch rays of whistler mode waves with variable frequencies and wave normal angles. We will use a ray-tracing technique of *Shklyar and Jiricek* [2000] and *Shklyar et al.* [2004] which was developed for whistler mode propagation studies in the magnetosphere.

[22] The ray tracing procedure is based on a dispersion relation in cold magnetized plasmas, which is valid only for the frequency range $\omega_{ci} << \omega \leq \omega_{ce}\cos\theta$, where ω_{ci} is the ion cyclotron frequency. The effect of ions is negligible in the frequency range under consideration. We use the dipole model for the magnetic field where the dipole moment has been adjusted in such a way that the electron cyclotron frequency corresponds to the observed value ($\omega_{ce}/2\pi$ = 12.6 kHz) at the spacecraft position. Since the ray tracing technique is used in the plasma trough outside the plasmasphere, the plasma density is approximated by a gyrotropic distribution of the plasma density n, $n \propto \omega_{rmp}^2 \propto \omega_{ce}^x$ (where we assume x = 1). The coefficient of proportionality has been adjusted to obtain the measured value of the plasma frequency ($\omega_p/2\pi$ = 42 kHz) at the spacecraft position.

[23] We limit our analysis to a two-dimensional case, in a single magnetic meridian plane. That means that the wave vector is fully described by its absolute value (wave number) and by the polar angle θ, which is positive if the wave vector is directed towards higher L shells and negative, if the wave vector is oriented to lower L shells. The azimuthal angle ϕ can thus only have two values in our case, 0° and 180°, respectively.

[24] Using the rays which illuminate the spacecraft we will construct the simulated combinations of frequencies and times of arrival. We then check if it is possible to adjust the free parameters of this simulation to fit the observed frequency-time spectrograms (Figure 1) and we will estimate the corresponding resonant electron energies. The ray-tracing calculation uses experimentally determined background conditions corresponding to the observation in Figure 1.

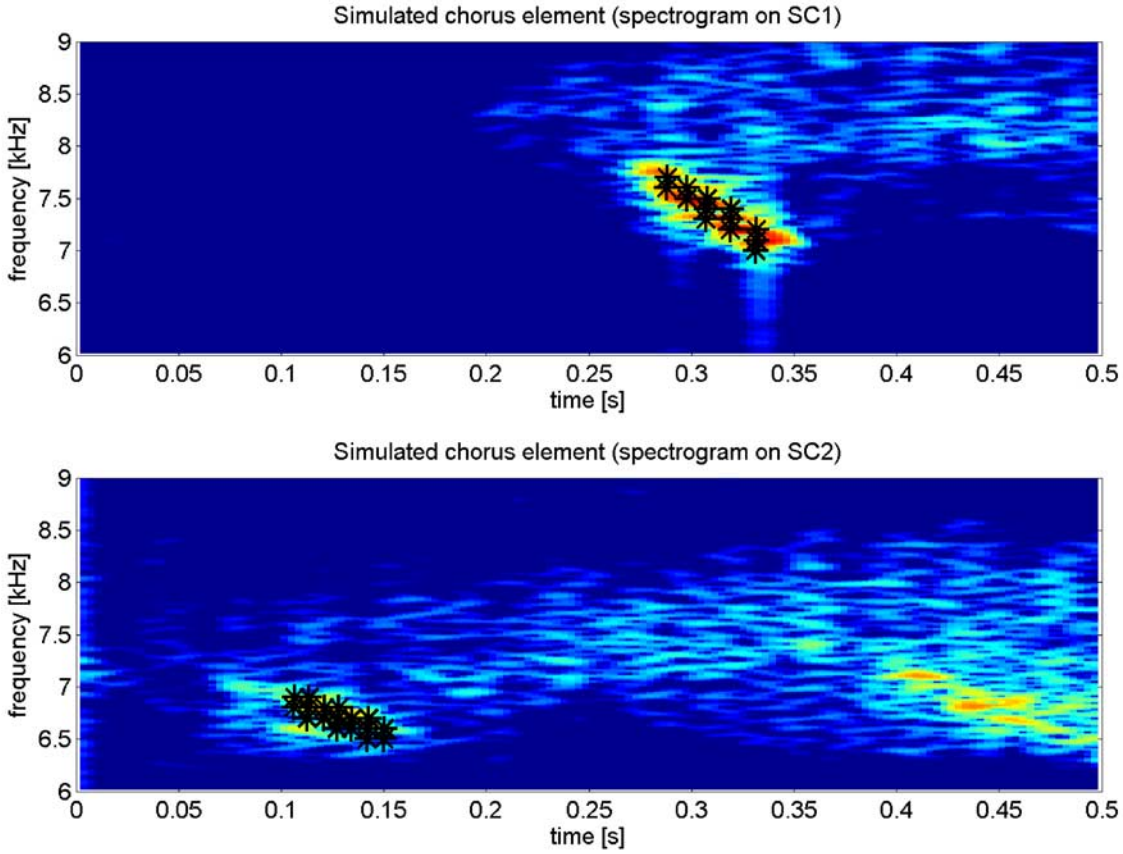

Figure 3. Simulation results are shown by black symbols for falling elements observed on 27 November 2000 at the location of Cluster 1 (SC1) and Cluster 2 (SC2). Zero time corresponds to 1313:43.2 UT. A scenario based on increasing wave normal angle presented in Figure 2 has been used. Two areas, shown by black rectangles on Figure 1, are plotted as frequency-time spectrograms under the simulation results, conserving the observed timing and frequency ranges. The color-coded range of power-spectral densities is the same as in Figure 1. The wave normal angle θ has been increased with time in such a way that the results of simulation fit the observation (see the text in section 4.1). The results of simulation for a particular time (value of θ) are marked by asterisks connected by a black line.

4.1. Falling Elements

[25] Figure 2 presents an illustration of ray-tracing for a source mechanism corresponding to the observation of falling elements. In this case, a frequency bandwidth of $\sim$0.7 kHz is emitted from a point source at L = 3.88 and a magnetic latitude of 1°, sweeping toward higher frequencies from a band between 6.5 and 7.2 kHz to a band between 7.0 and 7.7 kHz, in a time span of 250 ms. The emission is only over a very narrow range ($\approx$3 degrees) of the wave normal angle θ between the wave vector and the background magnetic field. During the 250-ms time span this narrow emission cone varies in angle θ from $\sim$0.25 θ_R to $\sim$0.65 θ_R, where $\cos\theta_R = \omega/\omega_{ce}$ is an approximation for the whistler mode resonance angle θ_R where $k_{||} \rightarrow \infty$ according to (2); θ_R thus varies with frequency inside the emitted band from $\approx$59° at 6.5 kHz down to $\approx$52° at 7.7 kHz.

[26] As a result of this sweep in θ, first one spacecraft is illuminated and then the other. Although frequency is varied as a function of time in this example, the predominant effect is that due to the wave normal angle variation. Note that this θ variation is not linear with time, to account for the different slopes of elements on the different spacecraft in Figure 3. However, for the range of angles used in this example, it was not necessary for θ to reach values close to resonance cone, where the resonant electron energy and the wave dispersion properties vary drastically with even a slight variation in wave normal angle.

[27] A comparison of the ray-tracing calculation with the observed chorus elements is presented in Figure 3 in the form of a frequency-time spectrogram. Two measured spectrograms from the two Cluster spacecraft are shown with the simulation results overplotted as a series of asterisks at discrete frequencies and times. The observed timing, frequency ranges, and frequency drift of the observed elements are reproduced quite well by the simulation. Although a point-like source was used in our simulation, we expect that the real source extends up to several thousands of kilometers along the field line and $\sim$10 to 100 km across the field line.

[28] Different frequencies can be generated in different subregions along the field line in the case of such an extended source. To fit the observations, the time-varying values of wave normal angles in each subregion would then have values which would be different from the values used

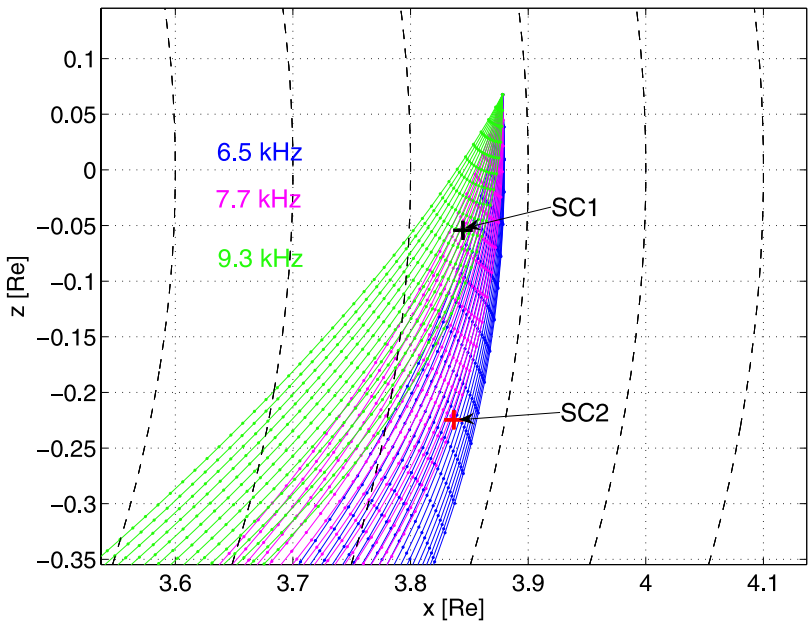

Figure 4. A schematic view in meridian plane of the chorus source used in the ray tracing simulation (solid lines) for rising elements from Figure 1. The dashed lines represent dipole magnetic field lines. We use a wide interval of emission angles θ from 0° to 0.67 θ_R (see text) for waves with frequency increasing from 6.5 kHz to 9.3 kHz in 620 ms.

in our simulation (Figures 2 and 3). Nevertheless, these values can be chosen in such a way that the results of the simulation are the same. Therefore the solution is not unique.

4.2. Rising Elements

[29] In the case of the fuzzy rising elements observed in Figure 1, a given frequency within an element is observed at almost the same time on both satellites. This suggests that the waves are emitted over a larger span of wave normal angles than that used in the previous example and that the increase of the frequency with time of the source emission becomes a more important effect than the change of the wave normal angle with time which was the case with the previous example. We have checked this by attempting to model this case with a simultaneous emission in the entire frequency range with a large span of wave normal angles and were not able to reproduce the observations solely from propagation effects even if the higher frequencies were generated further away from the point of observation (within a reasonable distance no more than a few degrees from the equator). The estimated group velocity is simply too large to yield the observed chorus element slopes. This leads to the conclusion that most of the observed rising element frequency variation with time is generated within the source and is not due to propagation effects.

[30] The character of the observed rising elements is that of fairly noisy blobs, rather than sharp rising tones, but for this case, we limited ourselves to the simulation of a characteristic rising slope. An example of the ray-tracing for three frequencies emitted from the point source at L = 3.88 and a magnetic latitude of 1° is presented in Figure 4. As discussed above, in this case, it is the frequency variation with time (from 6.5 kHz to 9.3 kHz in 620 ms) that dominates over the wave normal angle variation with time. We use a large interval of wave normal angles from 0° to 0.67 θ_R, which varies only as a consequence of variation of the resonance angle θ_R with frequency (from ≈58° at 6.5 kHz to ≈41° at 9.3 kHz). As before, it was not necessary to use wave normal angles near the resonance cone.

[31] The comparison of the measured chorus elements to the results from the ray tracing simulation for this case is shown in Figure 5. Two frequency-time spectrograms recorded by the two Cluster spacecraft (from Figure 1) are shown with simulation results for discrete frequencies and arrival times overplotted as asterisks. As in the previous case, the simulation well reproduces the observed characteristic frequency slope.

4.3. Energies of Resonant Electron Populations

[32] We now investigate the energies of the electrons which could cause the chorus emissions properties we have simulated. Since the first-order cyclotron resonance condition (1) defines only the parallel velocity of the electrons, we have to select an equatorial pitch angle of the resonant electron population to estimate the electron energies. The equatorial pitch angle determines the altitude of the magnetic mirror point of the electrons. For the present study, we have chosen the mirror point for the electron population that we assume drives the chorus emission to have an altitude of 500 km. This mirror point was chosen because it gives a pitch angle for the resonant electrons which is at the edge of the loss cone where we expect there to be a source of free energy for the wave growth. The electrons that are close to the loss cone have relatively low resonant energies, and we can thus consider the resonance condition in a simple nonrelativistic form where we assume $\gamma = 1$ in (1). The relativistic effects can be, however, very important for resonant electrons at pitch angles close to 90° [see *Horne and Thorne*, 2003].

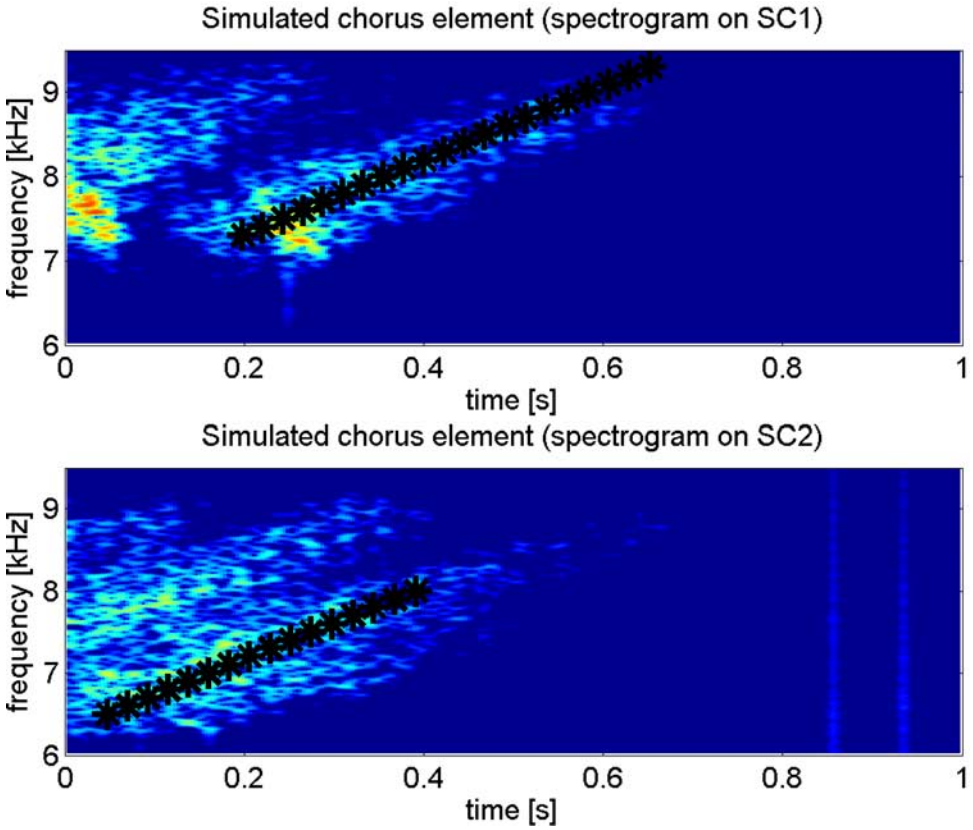

Figure 5. Simulated rising chorus element as observed at the location of SC1 and SC2 (black symbols). Zero time corresponds to 1313:44 UT (on 27 November 2000). A mechanism based on increasing frequency in time, (presented in Figure 4) was applied. Two frequency-time intervals, shown by white rectangles on Figure 1 are plotted as frequency-time spectrograms under the simulation results, conserving the observed timing and frequency ranges. The color-coded range of power-spectral densities is the same as in Figure 1. The slopes of simulated elements in frequency-time space mainly result from the fact that rays of individual frequencies were differently time-delayed at their origins so that the simulation would fit the observation. At higher frequencies, higher time delays were applied with a slope of $\approx$0.22 s/kHz.

[33] The magnitude of the resonant electron velocity v can be determined from the resonant velocity and the location of the magnetic mirror point of electrons on the field line which drive the chorus emission. Conservation of the first adiabatic invariant along a dipole magnetic field line gives

$$v_{\parallel} = v\left(1 - \frac{\cos^6 \lambda_m}{\sqrt{1+3\sin^2 \lambda_m}} \frac{\sqrt{1+3\sin^2 \lambda}}{\cos^6 \lambda}\right)^{\frac{1}{2}} \qquad (3)$$

where λ is the magnetic latitude of the generation region, and λ_m is the magnetic latitude of the mirror point, where the parallel velocity goes to zero, and is defined by:

$$R = L\cos^2 \lambda_m \ , \qquad (4)$$

where R is radial distance of the mirror point in Earth radii ($\sim$1.08 R_E for 500 km above the Earth), and L is the McIlwain parameter of the corresponding magnetic field line.

[34] For the values of the frequency and wave numbers used in the simulation results discussed in the previous sections, we have used (3) to determine the energies of the resonant electrons. This range of resonance energies is shown in Figure 6. According to the assumptions we have used (and described above), a band of available energies of unstable electron populations is needed. The energy interval for falling elements of 2–5 keV (shown in the blue dashed box) is narrower than the 500 eV to 5 keV range (shown with the black dashed line) for the rising elements. This is because the falling elements observed in our case occupy a narrower frequency bandwidth. Note that this model cannot exclude the possibility of resonant electrons with different pitch angles and hence, different energies, participating in the generation process but this example does show that a reasonable range of resonant electron energies is consistent with our results.

[35] From the previous analysis, it is obvious that we have considered a relatively large span of wave normal

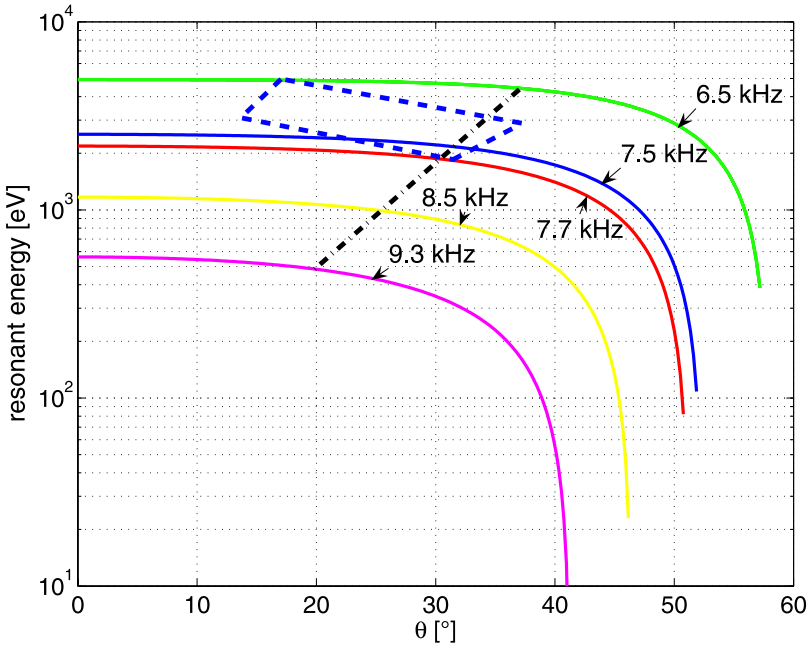

Figure 6. Resonant energies of electrons corresponding to the position of the source assumed in the ray-tracing simulations presented in Figures 3 and 5, as a function of the wave normal angle. The polygon drawn by a blue thick dash line indicates the range used for simulation of falling elements (Figure 3) and the thick black dash-dot line approximately indicates the range of resonant energies and the maximum wave normal angles that are important for the simulation of rising elements (Figure 5).

angles θ, including relatively large angles up to $\theta = 0.65\ \theta_R$. Particle measurements at energies below 25 keV are not available for this case, so we are unable to provide an experimental answer to the question whether the wave growth can be significant at these large angles. A linear cyclotron resonance growth usually maximizes for parallel propagation, whereas Landau damping is usually important for oblique whistler mode waves. *Brinca* [1972] showed that depending on the anisotropy and kinetic energy of hot electrons, the whistler waves can also be unstable for high values of θ. Considering that chorus is probably generated by a nonlinear mechanism, the analysis should be more complicated. Unfortunately, we have no measurement of wave normal angles for upper-band chorus on Cluster because multicomponent wave field measures are available only up to 4 kHz.

5. Discussion

[36] The two examples we have presented show that it is possible for a nonmoving source region which has both frequency and wave normal angle variation with time to reproduce the types of correlated chorus elements observed on the Cluster spacecraft. The specific values we have used to simulate these events are certainly not unique. There may be large variety of possible parameter choices for the two cases presented in the previous section which can produce similar signatures. By changing properly the wave normal angle θ and the frequency ω with time, we are able to simulate a large range of possible values of the frequency-time shift and dispersion. It demonstrates that this result does not depend on a single precise set of parameters to produce measured signatures.

[37] The sources of chorus elements most probably have a finite length along the field line. An approach very similar to our simple point-source approximation could be used to simulate these elongated field-aligned sources, but it is not expected that the essential result would change. Note also that we have chosen the initial conditions for the ray tracing simulation in such a way that the simulations fit the observations. For example, the location of the source has been selected as a free parameter and the evolution of wave normal angles and frequencies as a function of time has been constrained by the observations. Our justification in choosing this specific source location came from Polar and Cluster observations of a source region located close to the geomagnetic equator [*LeDocq et al.*, 1998; *Parrot et al.*, 2003b; *Santolík et al.*, 2004b, 2005].

[38] Our simulation shows what can happen if a chorus source has time-varying frequency and wave normal emission properties. It does not explain how such properties would arise. We cannot exclude the possibility that the real source of chorus elements has properties other than those assumed in this study. The presented solution is thus not unique also as concerns the underlying physical mechanism. With the data that are available in the presented case we are unable to verify if the unstable (or at least marginally unstable) electron population exist at energies under 25 keV which are assumed in this study. Neither we are able to show if the assumed higher wave normal angles can be detected in portions of the observed wave packet in the upper band of chorus. Without identification of the source

mechanism from direct measurements and/or without further theoretical considerations we cannot decide which of the possible models is better.

[39] An example of another possible mechanism could be a source moving transverse to the field lines (with a relatively low speed of ~300 km/s) which could lead to very similar effects on the simulated chorus elements. A source moving across L shells in the equatorial plane could also naturally explain the frequency shifts due to the variation of the local electron cyclotron frequency in the generation region. However the mechanism for such a motion is not clear. It seems not very likely that a transverse movement could be caused by $\mathbf{E} \times \mathbf{B}$ drift since it would require an unrealistically high quasi-static electric field (~100 mV/m). Perhaps, nonlinear wave-particle interactions of counterstreaming electrons and chorus waves propagating obliquely to the magnetic field lines could cause the transition of the individual sources to the lower L shells and could be consistent with these velocities. Analysis of possible mechanisms causing such a transverse motion is, however, beyond the scope of the present paper.

[40] Similar mechanisms could also be used for other observed chorus emissions showing the time and frequency shifts between corresponding chorus elements observed at different points in space. There is no principal feature of our model which would be specific to the upper-band chorus at frequencies above $\omega_{ce}/2$. With slightly different details it can thus also be used for lower-band chorus at frequencies below $\omega_{ce}/2$. In these cases it is possible to verify at least the presence of higher wave normal angles using the multicomponent measurements of the STAFF-SA instrument onboard Cluster. Analysis of such a case is under way and preliminary results show that, indeed, waves with higher wave normal angles can exist in the source region of chorus.

6. Conclusions

[41] We have presented a model which explains the frequency range variation and time shifts between corresponding chorus elements of upper-band chorus recorded on different Cluster spacecraft. We have shown that these shifts can be explained if the source emits waves in a relatively narrow interval of wave normal angles and varies both the wave normal angle and frequency during the generation of a single chorus element.

[42] In our specific case, the falling elements can be generated mainly as a result of the increasing wave normal angle of emitted waves, whereas rising elements could be observed predominantly as a result of the increasing emitted frequency. By varying these two quantities, we are able to simulate the observed frequency and time shifts. We have shown that a reasonable range of resonant electron energies is consistent with a given combination of increasing wave normal angles and frequencies emitted from the chorus source.

[43] We cannot prove that our model is definitively correct and that that other models are wrong, or vice versa. We only have shown in the present paper that one reasonable model for the observed chorus time and frequency variations is a fixed source with time varying emission properties. The task for future research is to decide which mechanism(s) really takes place.

[44] **Acknowledgments.** We thank R. Huff, J. Dowell, J. Seeberger, and other colleagues from the University of Iowa for the calibration and preprocessing of the WBD measurements. We acknowledge various discussions with D. Shklyar of IZMIRAN, Moscow. We thank P. Canu for estimating the plasma density. We acknowledge the access to the spin-resolution data of the FGM magnetic field experiment (PI E. Lucek) used for reference. This research was supported by the NASA Goddard Space Flight Center under grants NAG5-9974 and NNG04GB98G, and by the NSF award 0307319/KONTAKT grant ME 842. O. Santolík and J. Chum acknowledge additional support from the ESA PECS contract 98025 and GAAV grant IAA 301120601.

[45] Zuyin Pu thanks the reviewers for their assistance in evaluating this paper.

References

Anderson, R. R., and K. Maeda (1977), VLF emissions associated with enhanced magnetospheric electrons, *J. Geophys. Res.*, *82*, 135.

Andronov, A. A., and V. Y. Trakhtengerts (1964), Kinetic instability of the Earth's outer radiation belt, *Geomagn. Aeron.*, *4*, 233.

Balogh, A., et al. (2001), The Cluster magnetic field investigation: overview of in-flight performance and initial results, *Ann. Geophys.*, *19*, 1207.

Breneman, A. W., C. A. Kletzing, J. Chum, and O. Santolik (2007), Multi-spacecraft observations of chorus dispersion and source location, *J. Geophys. Res.*, doi:10.1029/2006JA012058, in press.

Brinca, A. L. (1972), On the stability of obliquely propagating whistlers, *J. Geophys. Res.*, *77*, 3495.

Décréau, P. M. E., et al. (2001), Early results from the Whisper instrument on Cluster: An overview, *Ann. Geophys.*, *19*, 1241.

Gurnett, D. A., and A. Bhatacharjee (2005), *Introduction to Plasma Physics With Space and Laboratory Applications*, Cambridge Univ. Press, New York.

Gurnett, D. A., R. L. Huff, and D. L. Kirchner (1997), The wide-band plasma wave investigation, *Space Sci. Rev.*, *79*, 195.

Gurnett, D. A., et al. (2001), First results from the Cluster wideband plasma wave investigation, *Ann. Geophys.*, *19*, 1259.

Helliwell, R. A. (1967), A theory of discrete emissions from the magnetosphere, *J. Geophys. Res.*, *72*, 4773.

Helliwell, R. A. (1969), Low-frequency waves in the magnetosphere, *Rev. Geophys.*, *7*, 281.

Horne, R. B., and R. M. Thorne (2003), Relativistic electron acceleration and precipitation during resonant interactions with whistler mode chorus, *Geophys. Res. Lett.*, *30*(10), 1527, doi:10.1029/2003GL016973.

Inan, U. S., M. Platino, T. F. Bell, D. A. Gurnett, and J. S. Pickett (2004), Cluster measurements of rapidly moving sources of ELF/VLF chorus, *J. Geophys. Res.*, *109*, A05214, doi:10.1029/2003JA010289.

Kennel, C. F., and H. E. Petschek (1966), Limit on stable trapped particle fluxes, *J. Geophys. Res.*, *71*, 1.

LeDocq, M. J., D. A. Gurnett, and G. B. Hospodarsky (1998), Chorus source locations from VLF Poynting flux measurements with the Polar spacecraft, *Geophys. Res. Lett.*, *25*, 4063.

Nunn, D., Y. Omura, H. Matsumoto, I. Nagano, and S. Yagitani (1997), The numerical simulation of VLF chorus and discrete emissions observed on the Geotail satellite using a Vlasov code, *J. Geophys. Res.*, *102*, 27,083.

Omura, Y., and D. Summers (2006), Dynamics of high-energy electrons interacting with whistler mode chorus emissions in the magnetosphere, *J. Geophys. Res.*, *111*, A09222, doi:10.1029/2006JA011600.

Parrot, M., O. Santolik, N. Cornilleau-Wehrlin, M. Maksimovic, and C. Harvey (2003a), Magnetospherically reflected chorus waves revealed by ray tracing with Cluster data, *Ann. Geophys.*, *21*, 1111.

Parrot, M., O. Santolík, N. Cornilleau-Wehrlin, M. Maksimovic, and C. Harvey (2003b), Source location of chorus emissions observed by Cluster, *Ann. Geophys.*, *21*, 473.

Parrot, M., O. Santolík, D. Gurnett, J. Pickett, and N. Cornilleau-Wehrlin (2004), Characteristics of magnetospherically reflected chorus waves observed by Cluster, *Ann. Geophys.*, *22*, 2597.

Santolík, O., and D. A. Gurnett (2003), Transverse dimensions of chorus in the source region, *Geophys. Res. Lett.*, *30*(2), 1031, doi:10.1029/2002GL016178.

Santolík, O., D. A. Gurnett, J. S. Pickett, M. Parrot, and N. Cornilleau-Wehrlin (2003), Spatio-temporal structure of storm-time chorus, *J. Geophys. Res.*, *108*(A7), 1278, doi:10.1029/2002JA009791.

Santolík, O., D. A. Gurnett, and J. S. Pickett (2004a), Multipoint investigation of the source region of storm-time chorus, *Ann. Geophys.*, *22*, 2555.

Santolík, O., D. A. Gurnett, J. S. Pickett, M. Parrot, and N. Cornilleau-Wehrlin (2004b), A microscopic and nanoscopic view of storm-time chorus on 31 March 2001, *Geophys. Res. Lett.*, *31*(4), L02801, doi:10.1029/2003GL018757.

Santolík, O., D. A. Gurnett, J. S. Pickett, M. Parrot, and N. Cornilleau-Wehrlin (2005), Central position of the source region of storm-time chorus, *Planet. Space Sci.*, *53*, 299.

Shklyar, D. R., and F. Jiricek (2000), Simulation of nonducted whistler spectrograms observed aboard the Magion 4 and 5 satellites, *J. Atmos. Terr. Phys.*, *62*, 347.

Shklyar, D. R., J. Chum, and F. Jiricek (2004), Characteristic properties of Nu whistlers as inferred from observations and numerical modelling, *Ann. Geophys.*, *22*, 3589.

Trakhtengerts, V. (1995), Magnetosphere cyclotron maser: backward wave oscillator generation regime, *J. Geophys. Res.*, *100*, 17,205.

Trakhtengerts, V. (1999), A generation mechanism for chorus emission, *Ann. Geophys.*, *17*, 95.

Tsurutani, B. T., and E. J. Smith (1974), Postmidnight chorus: A substorm phenomenon, *J. Geophys. Res.*, *79*, 118.

O. Santolík, Faculty of Mathematics and Physics, Charles University V, Holešovičkách 2, Prague, CZ-18000 Czech Republic. (ondrej.santolik@mff.cuni.cz)

J. Chum, Institute of Atmospheric Physics, Bocni II/1401, CZ-14131 Praha 4, Czech Republic. (jachu@ufa.cas.cz)

A. W. Breneman, D. A. Gurnett, C. A. Kletzing, and J. S. Pickett, Department of Physics and Astronomy, University of Iowa, Iowa City, IA 52242-1479, USA. (aaron-breneman@uiowa.edu; donald-gurnett@uiowa.edu; craig-kletzing@uiowa. edu; pickett@uiowa.edu)